A BLOCH BAND BASED LEVEL SET METHOD FOR COMPUTING THE SEMICLASSICAL LIMIT OF SCHRÖDINGER EQUATIONS

HAILIANG LIU AND ZHONGMING WANG

Abstract. A novel Bloch band based level set method is proposed for computing the semiclassical limit of Schrödinger equations in periodic media. For the underlying equation subject to a highly oscillatory initial data, a hybrid of the WKB approximation and homogenization leads to the Bloch eigenvalue problem and an associated Hamilton-Jacobi system for the phase in each Bloch band, with the Bloch eigenvalue be part of the Hamiltonian. We formulate a level set description to capture multi-valued solutions to the band WKB system, and then evaluate total homogenized density over a sample set of bands. A superposition of band densities is established over all bands and solution branches when away from caustic points. The numerical approach splits the solution process into several parts: i) initialize the level set function from the band decomposition of the initial data; ii) solve the Bloch eigenvalue problem to compute Bloch waves; iii) evolve the band level set equation to compute multi-valued velocity and density on each Bloch band; iv) evaluate the total position density over a sample set of bands using Bloch waves and band densities obtained in step ii) and iii), respectively. Numerical examples with different number of bands are provided to demonstrate the good quality of the method.

Contents

1. Introduction

In this paper we are concerned with numerical computation of physical observables to the linear Schrödinger equation

$$i\epsilon\partial_t\psi^\epsilon = -\frac{\epsilon^2}{2}\partial_x\left(b\left(\frac{x}{\epsilon}\right)\partial_x\psi^\epsilon\right) + V\left(\frac{x}{\epsilon}\right)\psi^\epsilon + V_e(x)\psi^\epsilon, \quad x\in\mathsf{IR},\ t\in\mathsf{IR}^+, \tag{1.1}$$

Date: Revision, September 22, 2008.

Key words and phrases. Schrödinger equation, Bloch waves, homogenization, semi-classical limit, level set method.

subject to the highly oscillatory function as initial data

$$\psi^\epsilon(0,x) = e^{iS_0(x)/\epsilon} g\left(x, \frac{x}{\epsilon}\right), \quad \epsilon \ll 1. \tag{1.2}$$

Here ψ^ϵ is the complex wave field, and ϵ is a re-scaled Planck constant. Both $b(y) > 0$ and $V(y)$ are smooth and periodic with respect to the regular lattice $\Gamma = 2\pi\mathbb{Z}$, i.e.,

$$b(y+2\pi) = b(y), \quad V(y+2\pi) = V(y), \quad \forall y \in \mathbb{R}. \tag{1.3}$$

The external potential V_e is a given smooth function.

This type of Schrödinger equations is a fundamental model in solid-state physics [2], and also models the quantum dynamics of Bloch electrons subjected to an external field. This problem has been studied from a physical, as well as from a mathematical point of view in, e.g., [1, 7, 30, 36, 41], resulting in a profound understanding of the novel dynamical features. An essential feature of the model, regardless of the point-of-view taken, is the energy band structure imposed on the model [6]. The mathematical asymptotic analysis as $\epsilon \to 0$ combining both semiclassical and homogenization limits has been a subject of intensive study in past decades, see e.g., [3, 5, 13, 24, 31, 39].

In the semiclassical regime, where ϵ is small, the external potential $V_e(x)$ varies at larger spatial scales than periodic potential $V(y)$ does and can be considered weak compared with periodic field. The wave function ψ^ϵ and the related physical observables become oscillatory of wave length $O(\epsilon)$. A direct simulation of (1.1) using the Bloch wave decomposition was recently developed, see e.g. [19], improving mesh sizes up to order $O(\epsilon)$. However, this system involves several different sources of oscillations, making direct numerical simulation prohibitively costly in the semiclassical regime.

A more realistic approach is to explore an asymptotic model by passing $\epsilon \to 0$. The periodic structure calls for the two scale expansion method [5, 18] in which the electron coordinate $y = \frac{x}{\epsilon}$ and the space variable x are regarded as independent variables.

$$\psi^\epsilon = A^\epsilon(t,x,y)\, e^{iS(t,x)/\epsilon},$$

in which the amplitude A^ϵ is assumed to admit an asymptotic expansion of the form

$$A^\epsilon(t,x,y) \sim A_0(t,x,y) + \epsilon A_1(t,x,y) + \epsilon^2 A_2(t,x,y) + \cdots.$$

The insertion of the above ansatz into (1.1) gives, to the leading orders of ϵ, a band Hamilton-Jacobi equation for the phase S and the transport equation for the amplitude ρ:

$$S_t + E(S_x) + V_e(x) = 0, \tag{1.4}$$

$$\rho_t + (E'(S_x)\rho)_x = 0, \tag{1.5}$$

where $E(k)$ is determined by solving the Bloch eigenvalue problem

$$H(k,y)z(k,y) = E(k)z(k,y), \quad z(k,y+2\pi) = z(k,y), \tag{1.6}$$

where

$$H(k,y) := \frac{1}{2}(-i\partial_y + k)[b(y)(-i\partial_y + k)] + V(y)$$

is a differential operator parameterized by k.

Singularity formation (S_x becomes discontinuous) in solutions of (1.4) is a generic phenomena even when the initial phase is smooth. Before the singularity formation, the

classical theory in [5] asserts that the wave function can be recovered by a superposition of wave patterns on each band

$$\left\| \psi^\epsilon(t,\cdot) - \sum_n \sqrt{\rho_n}(t,\cdot) z_n \left((S_n)_x, \frac{x}{\epsilon} \right) \exp\left(\frac{i S_n(t,\cdot)}{\epsilon} \right) \right\|_{L^2(\mathbb{R})} \sim \mathcal{O}(\epsilon).$$

After the singularity formation standard schemes using shock capturing ideas will select the viscosity solution [10, 11], which is inadequate in this context for describing the relevant physical phenomena. Multi-valued solutions for (1.4) are physically relevant ones. The first attempt to compute multi-valued solutions for (1.1) with $b(y) \equiv 1$ was due to [15], using so called K-branch solutions, see also subsequent works [14, 16].

Phase space based geometric methods were first introduced for tracking wave fronts in geometric optics, such as the segment projection method [12] and the level set method [34, 9, 38, 8]. More recently, a level set framework has been developed for computing multi-valued phases in the *entire physical domain* in [8, 22, 25, 21, 20]; main development has been summarized in the review article [26]. A key idea is to represent the n-dimensional bi-characteristic manifold of the Hamilton-Jacobi equation in phase space by an implicit vector level set function. Further developments are geared at handing more complex potentials or recovery of the original wave field, see [23, 27, 28, 29].

The aim of this paper is to extend the level set method of [8, 21] for linear Schrödinger equations to solve (1.1)-(1.2) with periodic structures. We formulate level set description to solve the banded WKB system (1.4)–(1.5) and then compute total averaged density over a sample set of Bloch bands. In order to illustrate the level set method developed in this paper, we let $\phi(t,x,k)$ be a function in phase space $(x,k) \in \mathbb{R}^2$, whose zero level set determines the multi-valued phase gradient $u = S_x$, i.e.,

$$u(t,x) \in \{k| \quad \phi(t,x,k) = 0\}, \quad (t,x) \in \mathbb{R}^+ \times \mathbb{R}.$$

It is shown that on n^{th} Bloch band, ϕ solves

$$\phi_t + E_n'(k)\phi_x - V_e'(x)\phi_k = 0.$$

The initial data for the level set function $\phi(t,x,k)$ is selected to uniquely imbed the initial phase gradient into its zero set.

Following [29], we compute the multi-valued density by

$$\rho_n(t,x) \in \left\{ \frac{f(t,x,k)}{|\phi_k|} \Big| \quad \phi(t,x,k) = 0 \right\}, \quad (t,x) \in \mathbb{R}^+ \times \mathbb{R},$$

where f is determined by solving the band Liouville equation

$$\begin{aligned} f_t + E_n'(k) f_x - V_e'(x) f_k &= 0, \\ f(0,x,k) &= \rho_n(0,x). \end{aligned} \tag{1.7}$$

Here $E_n(k)$ is obtained from solving the associated Bloch eigenvalue problem (1.6), for which we apply a standard Fourier method.

The initial density on each band is calculated from $\psi^\epsilon(0,x)$ in (1.2) through a projection procedure,

$$\rho_n(0,x) = \frac{1}{2\pi} |a_n(x)|^2,$$

where

$$a_n(x) = \int_0^{2\pi} g(x,y)\bar{z}_n(\partial_x S_0, y)dy.$$

Considering the possible phase shift, the wave profile in each Bloch band takes the form

$$\psi_n^\epsilon(t,x) = \sum_{j=1}^{K_n} \sqrt{\rho_n^j(t,x)} z_n\left(u_n^j(t,x), \frac{x}{\epsilon}\right) \exp\left(\frac{iS_n^j(t,x)}{\epsilon}\right) \exp\left(\frac{i\pi}{4}\mu_n^j\right),$$

where the phase shift μ_n^j corresponds to the usual Keller-Maslov phase shift [32].

Finally, the total position density over all bands is evaluated using Bloch waves and multi-valued densities obtained on each band:

$$\bar{\rho}(t,x) = \sum_n \sum_{j=1}^{K_n} \rho_n^j.$$

Although the level set equation is formulated in phase space, the computational cost, when using a local level set method such as those in [33, 34, 37], is almost linear in the number of grid points in physical domain. In contrast to the method of using K-branch solutions in [15], the level set method developed here is simple and more robust especially when the number of solution branches increase.

The rest of this paper is organized as follows: in §2, we derive the level set algorithm and analyze the effective position density to be computed. §3 describes the numerical procedure in four steps. Finally in §4 a series of numerical tests is given to validate our level set algorithm.

2. Level Set Formulation

In this section we follow a hybrid of semiclassical approximation and homogenization to derive the Bloch eigenvalue problem and the Bloch banded WKB system for phase and amplitude, and then formulate the level set method for each Bloch band, followed by computation of position density over a sample set of Bloch bands.

2.1. Semi-classical homogenization and Bloch decomposition.

We now sketch the asymptotic procedure to derive a limiting model for the Schrödinger equation

$$i\epsilon\frac{\partial\psi^\epsilon}{\partial t} = -\frac{\epsilon^2}{2}\partial_x\left(b\left(\frac{x}{\epsilon}\right)\partial_x\psi^\epsilon\right) + V\left(\frac{x}{\epsilon}\right)\psi^\epsilon + V_e(x)\psi^\epsilon, \quad x \in \mathbb{R}, t \in \mathbb{R}^+ \tag{2.1}$$

$$\psi^\epsilon(x,0) = e^{iS_0(x)/\epsilon} g\left(x, \frac{x}{\epsilon}\right). \tag{2.2}$$

We use, as illustrated in [5, 18], the two scale expansion method in which the electron coordinate $y = \frac{x}{\epsilon}$ and the space variable x are regarded as independent variables. Thus consider the following equation in the independent variables (t, x, y):

$$i\epsilon\partial_t\psi = \left[-\frac{1}{2}(\partial_y + \epsilon\partial_x)\left(b\left(y\right)\left(\partial_y + \epsilon\partial_x\right)\right) + V\left(y\right) + V_e(x)\right]\psi. \tag{2.3}$$

Note that if we let $y = x/\epsilon$ in the solution $\psi(t,x,y;\epsilon)$ of (2.3) we recover the solution of (2.1).

We now look for approximate solutions of the following form

$$\psi(t,x,y;\epsilon) = e^{iS(t,x)/\epsilon}\left[A_0(t,x,y) + \epsilon A_1(t,x,y) + \cdots\right], \tag{2.4}$$

where $A_0, A_1, \cdots$ are required to be $2\pi-$periodic function in y. A substitution of this ansatz into (2.3), collecting terms which are the same order in ϵ, gives

$$0 = e^{iS(t,x)/\epsilon} \left[c_0(t,x,y) + \epsilon c_1(t,x,y) + \cdots\right], \tag{2.5}$$

where the first two coefficients are

$$c_0(t,x,y) = -\left[S_t + H(k(t,x),y) + V_e(x)\right] A_0, \quad k(t,x) = S_x(t,x), \tag{2.6}$$

$$c_1(t,x,y) = iLA_0 - \left[S_t + H(k(t,x),y) + V_e(x)\right] A_1. \tag{2.7}$$

Here we have set

$$H(k,y) = -\frac{1}{2}(\partial_y + ik)[b(y)(\partial_y + ik)] + V(y), \tag{2.8}$$

$$L = \partial_t - \frac{i}{2}\left[(\partial_y + ik)[b(y)\partial_x] + \partial_x[b(y)(\partial_y + ik)]\right]. \tag{2.9}$$

It is known [40] that for smooth $V(y)$ and $b(y) > 0$, $H(k,y)$ admits a complete set of (normalized) eigenfunctions z_n for each fixed k, in the sense that $\{z_n(k,y)\}_{n=1}^{\infty}$ form an orthonormal basis in $L^2(0,2\pi)$ for any fixed k. Let z_n be the normalized eigenfunction corresponding to the eigenvalue $E_n(k)$, then

$$\begin{aligned} H(k,y)z_n(k,y) &= E_n(k)z_n(k,y), \\ z_n(k,y+2\pi) &= z_n(k,y), \quad k \in \mathcal{B}, \quad y \in \mathbb{R}. \end{aligned} \tag{2.10}$$

Here k is confined to the reciprocal cell $\mathcal{B} = [-0.5, 0.5]$(or a Brillouin zone in physical literature)[5, 40]. Correspondingly there exists a countable family of real eigenvalues which can be ordered according to

$$E_1(k) \le E_2(k) \le \cdots \le E_n(k) \le \cdots, \quad n \in \mathbb{N},$$

including the respective multiplicity. The set $\{E_n(k) | \quad k \in \mathcal{B}\}$ is called the n^{th} energy band, which together with the corresponding Bloch functions characterizes the spectral properties of the operator $H(k,y)$. Standard perturbation theory shows that $E_n(k)$ is a continuous function of k and is real analytic in a neighborhood of any k such that

$$E_{n-1}(k) < E_n(k) < E_{n+1}(k).$$

From now on we will suppress the index n whenever no confusion is caused.

We can thus satisfy $c_0 = 0$ in (2.6) by choosing

$$S_t + E(S_x) + V_e(x) = 0 \tag{2.11}$$

and setting

$$A_0(t,x,y) = a(t,x)z(k(t,x),y).$$

Thus $c_1 = 0$ in (2.7) becomes

$$iLA_0 - (H(k,y) - E(k))A_1 = 0.$$

By the Fredholm alternative, this equation has a solution A_1 if and only if

$$\langle Lz, z\rangle = 0. \tag{2.12}$$

A substitution of $A_0 = a(t,x)z(k(t,x),y)$ into (2.12) leads to the following transport equation for a:

$$\partial_t a + \frac{1}{2}a\partial_x E'(k(t,x)) + \partial_x a E'(k(t,x)) + \beta a = 0, \tag{2.13}$$

with

$$\beta = (\partial_t z, z) - \frac{1}{2}\partial_x E'(k(t,x)) - \frac{i}{2}\langle((\partial_y + ik(t,x))[b(y)\partial_x z] + b(y)\partial_x(\partial_y + ik(t,x))[z], z\rangle.$$

We now turn to show that the above β is purely imaginary so that $\rho = |a|^2$ satisfies

$$\rho_t + (E'(S_x)\rho)_x = 0. \tag{2.14}$$

In fact, if we use H_k, then β can be recast as

$$\beta = \langle z_t, z\rangle - \frac{1}{2}\partial_x E'(k) + \langle H_k \cdot \partial_x z, z\rangle + \frac{k_x}{2}\langle b(y)z, z\rangle. \tag{2.15}$$

Let $E(k)$ be a simple eigenvalue, then $z(k,y)$ may be assumed analytic in k. Thus, differentiating $H(k,y)z = E(k)z$ with respect to k we have

$$[E'(k) - H_k]\, z = [H - E]z_k, \tag{2.16}$$

which upon taking inner product with z gives

$$E'(k) = \langle H_k z, z\rangle. \tag{2.17}$$

Here we have used the fact that $\langle z(k,\cdot), z(k,\cdot)\rangle = 1$ and $H - E$ is self-adjoint. Further we differentiate (2.17) with respect to x, and noting that H_k is self-adjoint, to obtain

$$\begin{aligned}\partial_x E'(k) &= \langle z, H_k \cdot \partial_x z\rangle + \langle H_k \cdot \partial_x z, z\rangle + \langle(\partial_x H_k)z, z\rangle \\ &= 2Re\langle H_k \cdot \partial_x z, z\rangle + k_x\langle b(y)z, z\rangle.\end{aligned}$$

This combined with $\langle z_t, z\rangle \in i\mathbb{R}$ (which follows from $\langle z, z\rangle = 1$) when inserted into (2.15) yields

$$Re(\beta) = 0.$$

The superposition principle for linear Schrödinger equations suggests that the wave function has an asymptotic description of the form

$$\psi^\epsilon(t,x) = \sum_{n=1}^{\infty} a_n(t,x) z_n\left(\partial_x S_n, \frac{x}{\epsilon}\right) e^{iS_n(t,x)/\epsilon} + \mathcal{O}(\epsilon), \tag{2.18}$$

where $S_n(t,x)$ satisfies the n^{th} band Hamilton-Jacobi equation (2.11) with $E = E_n$.

Upon these equations for density (2.14), phase (2.11) as well as the Bloch waves (2.10), we proceed to formulate our Bloch band based level set method.

2.2. **Bloch band based level set equation.** Once we obtain the WKB system on n^{th} Bloch band

$$\begin{aligned} S_t + E(S_x) + V_e(x) &= 0, \\ \rho_t + (E'(S_x)\rho)_x &= 0, \end{aligned}$$

the next task is to solve them numerically to obtain multi-valued solutions (here again band indexes are suppressed). Here, multi-valued phase shall be sought in order to capture the relevant physical phenomena.

Let $\phi(t,x,k)$ be a function in phase space, whose zero level set implicitly describes the phase gradient $\partial_x S(t,x)$, where $S(t,x)$ solves (2.11), then ϕ is proven to satisfy

$$\phi_t + E'(k)\phi_x - V_e'(x)\phi_k = 0, \tag{2.19}$$

$$\phi(0,x,k) = k - \partial_x S_0(x), \tag{2.20}$$

with $E'(k)$ being solved from (2.10). The multi-valued velocity is then given by

$$u(t,x) \in \{k| \quad \phi(t,x,k) = 0\}, \quad \forall (t,x) \in \mathbb{R}^+ \times \mathbb{R}.$$

The corresponding multi-valued density can be evaluated as suggested in [29]

$$\rho(t,x) \in \left\{ \frac{f(t,x,k)}{|\phi_k|} \middle| \quad \phi(t,x,k) = 0 \right\}, \quad \forall (t,x) \in \mathbb{R}^+ \times \mathbb{R}, \tag{2.21}$$

where f solves

$$f_t + E'(k) f_x - V_e'(x) f_k = 0, \tag{2.22}$$

$$f(0,x,p) = \rho_0(x), \tag{2.23}$$

where $\rho_0(x)$ is to be determined from the initial data $\psi^\epsilon(0,x)$, see (2.27). The averaged density can be evaluated as

$$\bar{\rho}(t,x) = \int_{-\infty}^{+\infty} f(t,x,k)\delta(\phi) dk. \tag{2.24}$$

Note that we need to compute $E'(k)$ in the level set equation, which may also be evaluated based on $\{z_n\}$ using (2.17).

Remark 1. *The above procedure can be easily extended to more general case. For instance the case with coefficient $b(x, x/\epsilon)$ and potential $V(x, x/\epsilon)$ with no separation of two scales. However, in such case the Bloch eigenvalue problem becomes spatial dependent:*

$$H(k,x,y)z(k,x,y) = E(k,x)z(k,x,y), \quad z(k,x,y) = z(k,x,y+2\pi), \quad \forall (k,x) \in \mathcal{B} \times \mathbb{R}.$$

A level set formulation in multi-dimensional case can be derived in a straightforward manner.

2.3. **Initial band configuration.** We now discuss the recovery of the initial band density $\rho_n(0,x)$ from the given initial data

$$\psi_0^\epsilon\left(x, \frac{x}{\epsilon}\right) = g\left(x, \frac{x}{\epsilon}\right) \exp(iS_0(x)/\epsilon), \tag{2.25}$$

with a real-valued phase $S_0 \in C^\infty(\mathbb{R})$ and a possible complex-valued amplitude $g(x,\cdot) \in L^2(\mathbb{R})$.

From (2.18) it follows that one needs only to decompose g as follows:

$$g(x,y) = \sum_{n=1}^{\infty} a_n(x) z_n(\partial_x S_0, y).$$

The orthonormality of $z_n(\partial_x S_0, y)$ leads to the following formula for a_n

$$a_n(x) = \int_0^{2\pi} g(x,y) \bar{z}_n(\partial_x S_0, y) dy.$$

The above decomposition ensures that

$$\int_0^{2\pi} |\psi_0^\epsilon(x,y)|^2 dy = \int_0^{2\pi} |g(x,y)|^2 dy = \sum_{n=1}^{\infty} |a_n|^2. \tag{2.26}$$

Hence $\rho_n(x)$ can be evaluated by

$$\rho_n = \frac{1}{2\pi} |a_n(x)|^2 \tag{2.27}$$

so that $\frac{1}{2\pi}\int_0^{2\pi}|\psi_0^\epsilon(x,y)|^2dy=\sum_n\rho_n$.

2.4. **Evaluation of position density.** In this section, we evaluate the position density and the wave field based on the quantities computed from the level set algorithm.

Let $\{u_n^j, j=1,\cdots,K_n\}$ be the multi-valued velocities, $\{S_n^j, j=1,\cdots,K_n\}$ and $\{a_n^j, j=1,\cdots,K_n\}$ be the corresponding phase and amplitude on n^{th} band, the wave function of two scales, associated with each u_n^j, is

$$\psi^\epsilon(t,x,y,u_n^j)=a_n^j(t,x)z_n(u_n^j(t,x),y)\exp\left(\frac{iS_n^j(t,x)}{\epsilon}\right).$$

The wave field on each band is thus calculated from its phase space counterpart as

$$\begin{aligned}\psi_n^\epsilon(t,x,y)&=\int\psi^\epsilon(t,x,y,k)\delta(\phi)\det(\phi_k)dk\\&=\sum_{j=1}^{K_n}\int\psi^\epsilon(t,x,y,k)\delta(k-u_j^n(t,x))dk\\&=\sum_{j=1}^{K_n}\psi^\epsilon(t,x,y,u_n^j)=\sum_{j=1}^{K_n}a_n^jz_n\left(u_n^j,y\right)\exp\left(\frac{iS_n^j}{\epsilon}\right).\end{aligned}\tag{2.28}$$

This wave function is periodic in the lattice scale y, we thus only calculate the averaged band density as

$$\bar\rho_n^\epsilon(t,x)=\frac{1}{2\pi}\int_0^{2\pi}|\psi_n^\epsilon(t,x,y)|^2dy.$$

Lemma 2.1. *Away from caustics we have*

$$\bar\rho_n^\epsilon(t,x)\rightharpoonup\frac{1}{2\pi}\sum_{j=1}^{K_n}|a_n^j|^2\quad as\quad\epsilon\to0.\tag{2.29}$$

Proof. By a direct calculation we have

$$2\pi\bar\rho_n^\epsilon(t,x)=\sum_{j=1}^{K_n}|a_n^j|^2+\sum_{j\neq j'}a_n^ja_n^{j'}\exp(i(S_n^j-S_n^{j'})/\varepsilon)\int_0^{2\pi}z_n(u_n^j,y)\bar z_n(u_n^{j'},y)dy.$$

The cross-terms over different j,j', denoted by $O_1(n)$, will converge, when away from caustics, to zero weakly as $\epsilon\to0$. In fact, for any smooth test-function Φ

$$\int_{\mathbb{R}}O_1\Phi(x)dx=\sum_{j\neq j'}\int_{\mathbb{R}}a_n^ja_n^{j'}\exp(i(S_n^j-S_n^{j'})/\varepsilon)\int_0^{2\pi}z_n(u_n^j,y)\bar z_n(u_n^{j'},y)dy\Phi(x)dx.$$

According to the stationary phase lemma*, the non-trivial contribution as $\epsilon \to 0$ comes from the stationary points of $S_n^j(t,x) - S_n^{j'}(t,x)$, i.e.,

$$\mathcal{A}_1 := \{x | u_n^j(t,x) = u_n^{j'}(t,x), \quad j \neq j'\}. \tag{2.30}$$

Note that for $x \in \mathcal{A}_1$, $\int z_n(u_n^j, y)\bar{z}_n(u_n^{j'}, y)dy = 1$. According to our level set construction this only happens at the caustic points where $j' = j+1$ (or $j-1$), and at such points $a_n^j = a_n^{j'}$, $S_n^j = S_n^{j'}$ and $\partial_x^2(S_n^j - S_n^{j'}) \neq 0$. These terms will weakly converge to

$$O_1(n) \rightharpoonup \sum_{x^* \in \mathcal{A}_1} |a_n^j(x^*)|^2 \sqrt{\frac{2\pi\epsilon}{|(\partial_x(u_n^j - u_n^{j'})(x^*)|}} e^{\frac{i\pi\mu_n^j}{4}},$$

where $\mu_n^j = 1$ or -1 depending on the sign change of $\partial_x(u_n^j - u_n^{j'})(x^*)$. However, at caustic points both $\partial_x u_n^j$ and $\partial_x u_n^j = -\phi_x/\phi_p$ become unbounded with different signs such that $|\partial_x(u_n^j - u_n^{j'})| = \infty$. On the other hand at caustics a_n^j also becomes unbounded. These together leave the above weak limit undefined at caustic points. □

We now consider all Bloch bands. Since the underlying equation is linear, the wave field over all bands is simply a superposition of wave filed on each band

$$\psi^\epsilon(t,x,y) = \sum_{n=1}^{\infty} \sum_{j=1}^{K_n} a_n^j z_n\left(u_n^j, y\right) \exp\left(\frac{iS_n^j}{\epsilon}\right).$$

Lemma 2.2. *Let the total density be defined as*

$$\rho^\epsilon(t,x) = \frac{1}{2\pi}\int_0^{2\pi} |\psi^\epsilon(t,x,y)|^2 dy. \tag{2.31}$$

Then away from caustics, we have

$$\rho^\epsilon(t,x) \rightharpoonup \frac{1}{2\pi}\sum_n \sum_{j=1}^{K_n} |a_n^j|^2 \quad as \quad \epsilon \to 0. \tag{2.32}$$

Proof. A direct calculation gives

$$\begin{aligned}
2\pi\rho^\epsilon(t,x) &= \sum_n \sum_{j=1}^{K_n} |a_n^j|^2 + \sum_n \sum_{j \neq j'} a_n^j \bar{a}_n^{j'} \exp(i(S_n^j - S_n^{j'})/\varepsilon) \int_0^{2\pi} z_n(u_n^j, y)\bar{z}_n(u_n^{j'}, y)dy \\
&+ \sum_{m \neq n} \sum_{j,j'} a_m^j a_n^{j'} \exp(i(S_n^j - S_m^{j'})/\varepsilon) \int_0^{2\pi} z_n(u_n^j, y)\bar{z}_m(u_m^{j'}, y)dy \\
&\equiv \sum_n \sum_{j=1}^{K_n} |a_n^j|^2 + Q_1 + Q_2.
\end{aligned}$$

As shown in Lemma 2.1 the term $Q_1 = \sum_n O_1(n) \rightharpoonup 0$ away from caustics.

*Let x^* be the critical point of the phase $\phi(x)$, $x \in \mathbb{R}$. For any integrable function $F(x)$, the following asymptotic formula holds

$$\int_{\mathbb{R}} F(x) e^{i\phi(x)/\epsilon} dx \simeq \sqrt{\frac{2\pi\epsilon}{|\phi_{xx}(x^*)|}} \exp\left(\text{sign}(\phi_{xx}(x^*))\frac{\pi i}{4}\right) \exp\left(\frac{i\phi(x^*)}{\epsilon}\right) F(x^*).$$

For the term Q_2 we explore the stationary phase lemma again. The only $O(1)$ contribution comes from the stationary points of $S_n^j(t,x) - S_m^{j'}(t,x)$, i.e.,

$$\mathcal{A}_2 := \{x | u_n^j(t,x) = u_m^{j'}(t,x), \quad m \neq n\}. \tag{2.33}$$

However for $x \in \mathcal{A}_2$, it holds

$$\int_0^{2\pi} z_n(u_n^j, y)\bar{z}_m(u_m^{j'}, y)dy = 0,$$

where we have used the fact $\langle z_n(k,\cdot), z_m(k,\cdot)\rangle = \delta_{mn}$ for any fixed k. Therefore, $Q_2 \rightharpoonup 0$ as $\epsilon \to 0$. The proof is thus complete. □

Based on Lemma 2.1 and 2.2, the total position density $\bar{\rho}(x)$ can be evaluated by

$$\bar{\rho}(x) = \sum_n \sum_{j=1}^{K_n} \rho_n^j, \tag{2.34}$$

where $\rho_n^j = \frac{1}{2\pi}|a_n^j|^2$ is given by (2.21).

Remark 2.3. The above analysis shows that in order to recover the wave field, one needs a caustic correction — the so called Keller-Maslov phase shift [32] such that

$$\psi^\epsilon(t,x) = \sum_n \sum_{j=1}^{K_n} a_n^j(t,x) z_n\left(u_n^j, \frac{x}{\epsilon}\right) \exp\left(\frac{iS_n^j}{\epsilon}\right) \exp\left(\frac{i\pi}{4}\mu_n^j\right). \tag{2.35}$$

However, this modified wave profile is valid only before and after caustics. To obtain a uniformly valid wave field a globally bounded a_n^j needs to be constructed. This will be considered in a future publication.

2.5. **2D Strang Splitting spectral method.** This section is to present a spectral scheme to compute the solution of (2.3), i.e.,

$$i\epsilon\partial_t\psi = \left[-\frac{1}{2}(\partial_y + \epsilon\partial_x)\left(b\left(y\right)\left(\partial_y + \epsilon\partial_x\right)\right) + V\left(y\right) + V_e(x)\right]\psi. \tag{2.36}$$

The computed solution will be used to compare with the solution computed from our level set method.

For simplicity, we assume $V_e(x)$ is a periodic function in $x \in [a,b]$. Then $\psi(t,x,y)$ is a periodic solution to (2.36) in both x and y. We choose spatial meshes

$$\Delta x = \frac{b-a}{J}, \quad \Delta y = \frac{2\pi}{P}$$

where both J and P are even integers. Let the grid points be (x_j, y_p)

$$x_j = a + j\Delta x, \quad j = 0, 1, \cdots J-1; \quad y_p = p\Delta y, \quad p = 0, \cdots, P-1.$$

Let $\phi_{j,p}(t)$ be the numerical approximation of $\phi(t, x_j, y_p)$.

Given $\phi_{j,p}(t)$ we shall compute $\phi_{j,p}(t+\Delta t)$. From t to $t+\Delta t$ we follow [4] to solve equation (2.36) by a Strang Splitting spectral method. For $j = 0, \cdots, J-1, \quad p =$

$0, \cdots, P-1$,

$$\psi^*_{j,p} = \exp\left(-\frac{i\Delta t}{2\epsilon}(V(y_p) + V_e(x_j))\right)\phi_{j,p}(t),$$
$$\hat{\psi}^{**}_{m,q} = \left(G\hat{\psi}^*\right)_{m,q}, \quad G \quad \text{is defined in (2.38) below,}$$
$$\psi^{**}_{j,p} = \frac{1}{JP}\sum_{m=-J/2}^{J/2-1}\sum_{q=-P/2}^{P/2-1}\hat{\psi}^{**}_{m,q}\exp\left(im\frac{2\pi(x_j-a)}{b-a} + iqy_p\right),$$

$$\psi_{j,p}(t+\Delta t) = \exp\left(-\frac{i\Delta t}{2\epsilon}(V(y_p) + V_e(x_j))\right)\psi^{**}_{j,p}. \tag{2.37}$$

Here $\hat{\psi}_{m,q}$, the Fourier coefficients of $\psi_{j,p}$, is defined as

$$\hat{\psi}_{m,q} = \sum_{j=0}^{J-1}\sum_{p=0}^{P-1}\psi_{j,p}\exp\left(-im\frac{2\pi(x_j-a)}{b-a} - iqy_p\right)$$

for $m = -\frac{J}{2}, \cdots, \frac{J}{2}-1$ and $q = -\frac{P}{2}, \cdots, \frac{P}{2}-1$.

We now determines the operator G as follows: we insert the Fourier series

$$\psi(t,x,y) = \sum_{m,q}\hat{\psi}_{m,q}(t)\exp\left(im\frac{2\pi(x-a)}{b-a} + iqy\right), \quad b(y) = \sum_q \hat{b}_q\exp(iqy),$$

into the equation spilt from (2.36):

$$i\epsilon\partial_t\psi = -\frac{1}{2}(\partial_y + \epsilon\partial_x)\left(b\left(y\right)(\partial_y + \epsilon\partial_x)\right)\psi,$$

and truncate to arrive the following ODE system

$$i\epsilon\frac{d}{dt}\hat{\psi}_{m,q} = \frac{1}{2}\sum_{q'=-P/2}^{P/2-1}\hat{\psi}_{m,q'}\hat{b}_{q-q'}\left(q + m\frac{2\pi\epsilon}{b-a}\right)\cdot\left(q' + m\frac{2\pi\epsilon}{b-a}\right), \quad q = -\frac{P}{2}, \cdots, \frac{P}{2}-1.$$

Introduce a $P \times P$ matrix $\hat{H}$ with entries as

$$\hat{H}_{r,s} = \hat{b}_{r-s}\left(r - \frac{P}{2} - 1 + m\frac{2\pi\epsilon}{b-a}\right)\cdot\left(s - \frac{P}{2} - 1 + m\frac{2\pi\epsilon}{b-a}\right).$$

The solution operator G is thus given as

$$(G\hat{\psi})_{m,q} = \left(\exp\left(\frac{-i\Delta t}{2\epsilon}H\right)(\hat{\psi}_{m,-P/2}, \cdots, \hat{\psi}_{m,P/2-1})^\top\right)_{q+P/2+1}. \tag{2.38}$$

If $b \equiv 1$, then operator G can be reduced to a simple formulation as

$$(G\hat{\psi}^*)_{m,q} = \exp\left(-\frac{i\Delta t}{2\epsilon}\left(q + m\frac{2\pi}{b-a}\epsilon\right)^2\right)\hat{\psi}^*_{m,q}.$$

3. Numerical Procedures

In this section, we first examine the Bloch waves numerically and then show how to implement the level set method developed in this paper. The solution process is carried out in following steps.

Step 1. Solving Bloch eigenvalue problem

We first evaluate $E_n(k)$ from a sequence of the eigenvalue problems (2.10)

$$V(y)z_n + \frac{1}{2}(-i\partial_y + k)\left[b(y)(-i\partial_y + k)z_n\right] = E_n(k)z_n, \tag{3.1}$$

where $E_n(k)$ is the n^{th} energy band, and $e^{iky}z_n$ is the n^{th} Bloch function with $k \in [-\frac{1}{2}, \frac{1}{2}]$. Since $z_n(k,y), b(y)$ and $V(y)$ are $2\pi-$periodic functions in y, we can expand them in Fourier series

$$V(y) = \sum_{q\in\mathbb{Z}} \hat{V}_q \exp(iqy), \quad \hat{V}_q = \frac{1}{2\pi}\int_0^{2\pi} V(y)\exp(-iqy)dy, \tag{3.2}$$

$$b(y) = \sum_{q\in\mathbb{Z}} \hat{b}_q \exp(iqy), \quad \hat{b}_q = \frac{1}{2\pi}\int_0^{2\pi} b(y)\exp(-iqy)dy, \tag{3.3}$$

$$z_n(k,y) = \sum_{q\in\mathbb{Z}} \hat{z}_{n,q} \exp(iqy), \quad \hat{z}_{n,q} = \frac{1}{2\pi}\int_0^{2\pi} z_n(k,y)\exp(-iqy)dy. \tag{3.4}$$

Insertion of these into (3.1) leads to

$$\frac{1}{2}\sum_{q\in\mathbf{Z}}(k+m)(k+q)\hat{a}_{m-q}\hat{z}_{n,q} + \sum_{q\in\mathbf{Z}}\hat{V}_{m-q}\hat{z}_{n,q} = E_n(k)\hat{z}_{n,m}, \quad \forall m \in \mathbb{Z}. \tag{3.5}$$

Extracting $2N+1$ terms for $q \in \{-N, \cdots, N\}$, we have the corresponding matrix $H = (H_{m,q})$ of the eigenvalue problem with

$$H_{m,q} = \frac{1}{2}(k+m)(k+q)\hat{a}_{m-q} + \hat{V}_{m-q}, \quad -N \le m, q \le N.$$

This is a Hermitian matrix satisfying

$$H\begin{bmatrix} (\hat{z}_n)_{-N} \\ \vdots \\ (\hat{z}_n)_N \end{bmatrix} = E_n(k)\begin{bmatrix} (\hat{z}_n)_{-N} \\ \vdots \\ (\hat{z}_n)_N \end{bmatrix}. \tag{3.6}$$

Note that by a transform of $\tilde{z}_n(y) = z_n(k,y)e^{imy}$ in (3.1), we obtain an equivalent eigenvalue problem to (3.5) for $\tilde{z}_n$, which shows that the eigenvalue problem is invariant under any integer shift in k. Taking $m = 1$, we have the following relation,

$$E_n(k+1) = E_n(k), \quad z_n(k+1,y) = z_n(k,y), \tag{3.7}$$

which implies that the fundamental domain of dual lattice, $\overline{\mathcal{B}} = [-0.5, 0.5]$, is not restricted. Note that the eigen-matrix in (3.6) is independent of spatial grids and time, we only have to solve it once; therefore the computational complexity of this step is not a major concern. In our simulation, $N = 50 \sim 100$.

After solving the above Bloch eigenvalue problem at each grid point $\{k_i \in [-0.5, 0.5], i = -M_k, \cdots, M_k\}$ with mesh size Δk, we are equipped with discrete function values of $E_n(k_i)$.

We now evaluate $\{E_n'(k_i), i = -M_k, \cdots, M_k\}$ for any grid point k_i. A natural way of computing first order derivative to a certain order accuracy is by polynomial interpolation using nearby grid points. Note that, periodic boundary conditions are used due to the 1-periodicity of $E(k)$, (3.7). A second order approximation is

$$E'(k_i) = \frac{E(k_{i+1}) - E(k_{i-1})}{2\Delta k}, \tag{3.8}$$

and a fourth order approximation is given by

$$E'(k_i) = \frac{E(k_{i-2}) - 8E(k_{i-1}) + 8E(k_{i+1}) - E(k_{i+2})}{12\Delta k}. \tag{3.9}$$

Note that in this case, $E'(k)$ can also be computed from $z(k, y)$ by the integral (2.17).

Step 2. Bloch band based decomposition of initial data.
Given the WKB-type wave function

$$\psi^\epsilon\left(x, \frac{x}{\epsilon}\right) = g\left(x, \frac{x}{\epsilon}\right) \exp(iS_0(x)/\epsilon),$$

we compute the band density ρ_n defined in (2.27) by using different number of energy bands from the Bloch waves. We will check how many eigen-modes are needed to recover the density $\rho = \frac{1}{2\pi}\int_0^{2\pi} |\psi^\epsilon(x, y)|^2 dy$ at a desired accuracy. Here we measure the accuracy by L^1 error

$$error = ||\rho - \sum_{n=1}^{M} \rho_n||_{L^1}, \quad M = 2, 4, 6, 8, 10, \cdots. \tag{3.10}$$

The choice of M is studied numerically in Section 4.1. We find out that for smooth potential $V(x)$ and initial $\psi_0^\epsilon(x)$, 8 bands are sufficient for the numerical simulation.

Step 3. Solving the level set equation

$$\phi_t + E'(k)\phi_x - V_e'(x)\phi_k = 0, \tag{3.11}$$

subject to initial data (2.20).

We discretize space with uniform mesh size Δx and Δk, and use $\phi(t, x_i, k_j)$ to denote the grid function value. Let $\phi_{ij}(t) \approx \phi(t, x_i, k_j)$ be the numerical solution, computed from the upwind semi-discrete scheme

$$\frac{d}{dt}\phi_{ij}(t) = L(\phi_{ij}), \tag{3.12}$$

$$\begin{aligned} L(\phi_{ij}) := & -E'(k_j)\frac{(\phi_{ij})_x^+ + (\phi_{ij})_x^-}{2} + |E'(k_j)|\frac{(\phi_{ij})_x^+ - (\phi_{ij})_x^-}{2} \\ & -V_e'(x_i)\frac{(\phi_{ij})_k^+ + (\phi_{ij})_k^-}{2} + |V_e'(x_i)|\frac{(\phi_{ij})_k^+ - (\phi_{ij})_k^-}{2}, \end{aligned} \tag{3.13}$$

where $E'(k)$ was evaluated in **Step 1**. Higher order spatial approximation can be achieved by high order ENO reconstruction applied to both $\phi_x^\pm$ and $\phi_k^\pm$ respectively, see [35]. Here we use a second order ENO reconstruction in our simulation.

In time, a two-stage, second order Runge-Kutta method [17] is used

$$\begin{aligned} \phi_{ij}^* &= \phi_{ij}^n + \Delta t L(\phi_{i,j}^{(n)}), \\ \phi_{ij}^{n+1} &= \frac{1}{2}\phi_{ij}^n + \frac{1}{2}\left(\phi_{ij}^* + \Delta t L(\phi_{ij}^*)\right). \end{aligned} \tag{3.14}$$

Now,we briefly summarize the procedure here:

(i) Find high order approximation of $(\phi_{ij})^{\pm}_{x,k}$ using ENO, and $E'(k_j)$ using (3.8) or (3.9) at each grid point,
(ii) Solve (3.11) by using (3.12) and (3.14),
(iii) Project $\phi = 0$ onto $x - k$ plane to get S_x.

Note that in (ii), one may use interpolation to approximate $E'(k)$ when grid point of $E'(k_j)$ is not coincided with the grid point obtained in (3.8) or (3.9). In our computation, we simply choose the same grid points.

Step 4. Computing the density ρ.
We solve (2.22) with initial condition (2.23) using methods described in **step 3** in each band to obtain f_n for $n = 1, \cdots M$, where M is the number of bands to be sampled. M is taken to be 10 in our numerical tests in next section.

The position density is to be computed by

$$\begin{aligned} \bar{\rho}(t,x) &= \sum_{n=1}^{M} \int f_n(t,x,k)\delta(\phi_n)dk \\ &= \sum_{n=1}^{M} \sum_{k_i} f_n(t,x,k_i)\delta_\eta(\phi_n(t,x,k_i))\Delta k, \end{aligned} \tag{3.15}$$

where δ_η is an approximation of the $\delta-$function. Let χ denote the characteristic function, our choice is

$$\delta_\eta(\phi) = \frac{1+\cos(\pi\phi/\eta)}{2\eta}\chi_{[-\eta,\eta]}.$$

Finally, we compare the density obtained from (3.15) with

$$\rho(t,x) = \frac{1}{2\pi}\sum_{p=0}^{P-1} |\psi(t,x,y_p)|^2 \Delta y, \tag{3.16}$$

where $\psi(t,x,y)$ is computed by the Strang splitting spectral method (2.37) for different ϵ.

4. Numerical Examples

4.1. **Bloch band based initial decomposition.** We first examine the accuracy of the Bloch band decomposition of the initial data

$$\psi_0(x) = g(x, x/\epsilon)e^{iS_0(x)/\epsilon}, \quad \epsilon \ll 1,$$

in terms of Bloch functions $\{z_n\}$ obtained from (3.1) with $V(y) = \cos(y)$ and $b(y) \equiv 1$. This internal potential $V(y) = \cos(y)$ will be used in some numerical tests below.

The eigen-structure of this potential $V(y)$ and $b(y)$ is shown in Fig.1, in which we observe that all 5 eigenvalues are distinct for any $k \in \mathcal{B}$. It meets the assumption of the Bloch Band expansion in Section 2.

In all examples of this section the computation domain is chosen to be $(x,k) \in [0, 2\pi] \times [-0.5, 0.5]$ with 151×101 grid points and 101×101 eigen-matrix.

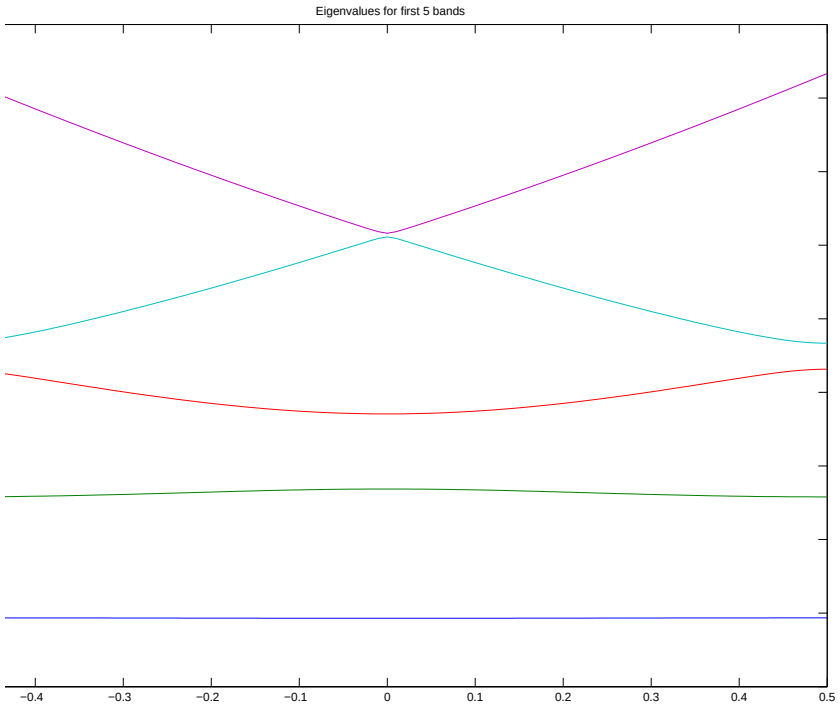

FIGURE 1. Eigenvalues for $V(y) = cos(y)$ and $b \equiv 1$ of n^{th} band, with $n = 1, \cdots, 5$ (bottom to top).

We compare the L^1 error of the Bloch decomposition, defined in (3.10), for the following data

$$(i) \qquad g(x,y) = \exp\left(\frac{-(x-\pi)^2}{2}\right), \quad S_0(x) = 0,$$

$$(ii) \qquad g(x,y) = \exp\left(\frac{-(x-\pi)^2}{2}\right), \quad S_0(x) = -0.3\cos(x),$$

$$(iii) \qquad g(x,y) = \exp\left(\frac{-(x-\pi)^2}{2}\right)\cos(y), \quad S_0(x) = 0.$$

A comparison table is given below.

# of bands	4	6	8	10	12
L^1 error of (i)	0.032843	0.009905	0.009879	0.009879	0.009879
L^1 error of (ii)	0.017008	0.008111	0.008101	0.008101	0.008101
L^1 error of (iii)	0.691181	0.062764	0.059332	0.059329	0.059329

From the above table we see that 8 bands give a good approximation with L^1 error of the order of 10^{-2}, with $\Delta x = 2\pi/150$ and $\Delta k = 1/100$. Including more bands does not seem to improve the accuracy of decomposition. Fig.2 shows a comparison between the

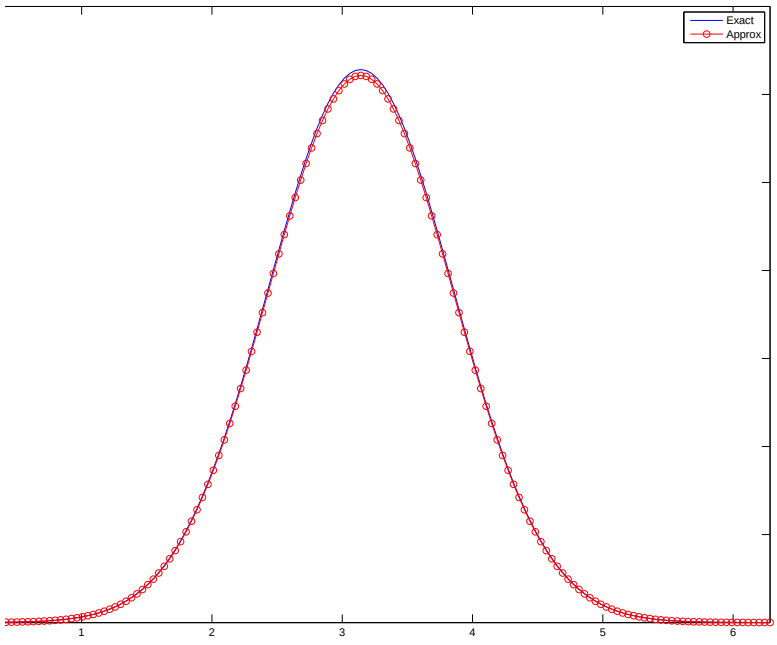

FIGURE 2. Initial data (iii), Bloch decomposition of initial density, exact density vs approximation with 8 bands

exact density and an approximation using 8 bands of data (iii). We see that they match very well. This tells that, in solving level set equation (3.11), only a few bands are needed, which makes our level set method more practical.

4.2. **Numerical examples.** We consider the periodic potential

$$V = \cos\left(\frac{x}{\epsilon}\right)$$

for all examples below.

Example 1. $b = 1$, $V_e = 0$ and

$$\psi^\epsilon(0,x) = \exp\left(-\frac{(x-\pi)^2}{2}\right)\exp\left(\frac{-0.3i\cos(x)}{\epsilon}\right).$$

This example is to compare total averaged density computed from our level set (LS) algorithm with the corresponding quantity in (3.16). From Fig.3, we observe that in these three plots each density computed by the level set algorithm predicts the correct trend as desired.

In what follows we shall test our level set algorithm for different choices of b and external potentials as well as of $z_n(k,y)$.

Example 2. $b \equiv 1$, $V_e = 0$, and

$$\psi^\epsilon(0,x) = e^{\frac{-0.3i\cos(x)}{\epsilon}} e^{-(x-\pi)^2} z_n(0.3\sin(x), x/\epsilon), \quad n = 3,4,5.$$

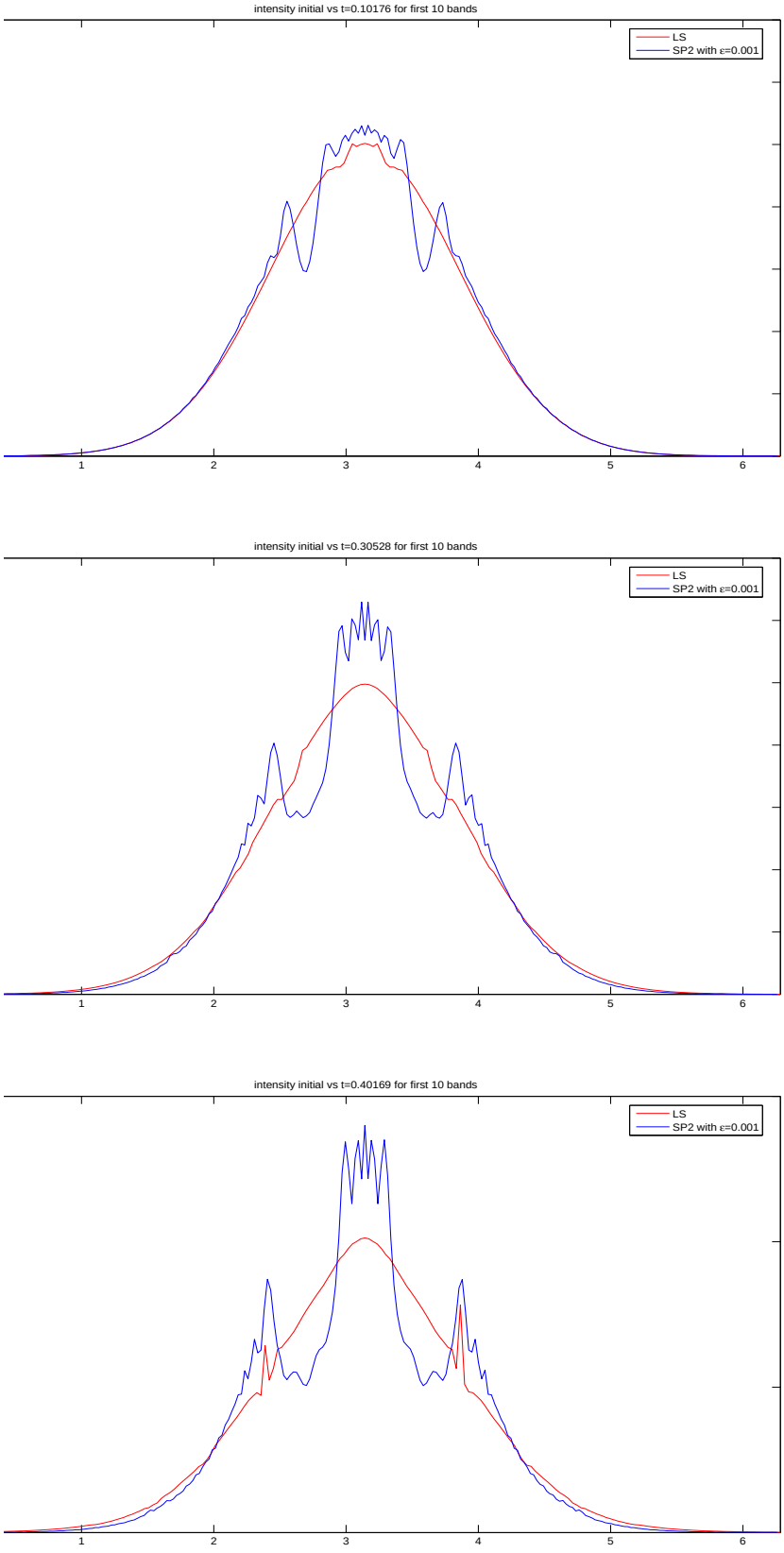

FIGURE 3. Example 1, homogenized density at different times

# of bands	4	6	8	10	12
L^1 error	0.004515	0.000967	0.000950	0.000950	0.000950

TABLE 1. L^1 error table for initial Bloch decomposition of example 4 with 101×101 grid points and 101 eigen-matrix.

This example is to test capacity of the level set algorithm to capture multi-valued velocities and associated densities in different bands.

From the Bloch eigenvalues given in Fig.1 we see that when $n = 3$, $E_3'(k)$ is positive when $k > 0$ and negative when $k < 0$; $|E_4(k)| \sim -2|k|$ and $|E_5(k)| \sim 2|k|$. Thus when initial velocity is a sine profile, both the third and fifth band will lead to multi-valued solutions to the corresponding equation for $u = S_x$:

$$u_t + E_n'(u)u_x = 0.$$

The forth band leads to a smooth rarefaction profile in u. The density is calculated as (3.15).

The case $n = 3$ is illustrated in Fig.4 for multi-valued velocity and averaged density at different times. From these figures we see that the density becomes infinite where the velocity has turns.

The case $n = 4$ is displayed in Fig. 5, in which we see that as the rarefaction appears around $x = \pi$, the averaged density tends to zero. Note that the multi-valued velocity at the boundaries are the waves from adjacent period, because of the periodic boundary condition.

When $n = 5$, multi-valuedness in velocity appears immediately when $t > 0$, see Fig.6.

Example 3. $b \equiv 1$, the harmonic potential $V_e = \frac{|x-\pi|^2}{2}$ and the initial data

$$\psi^\epsilon(0,x) = e^{\frac{-0.3i\cos(x)}{\epsilon}} e^{-\frac{(x-\pi)^2}{2}} z_5\left(0.3\sin(x), \frac{x}{\epsilon}\right).$$

This example is to show the level set method to be capable of dealing with nontrivial external potentials. In presence of a nontrivial V_e, both shapes and amplitudes of u will change, a larger computation domain may be needed so that the computed velocity remains to be observed in k direction. In Fig.7 we observe the motion of peaks in intensity, which corresponds to the location of turning points in velocity.

Example 4. $b = \frac{3}{2} + \sin(y)$, $V_e = 0$, and

$$\psi^\epsilon(0,x) = \exp\left(-\frac{(x-\pi)^2}{2}\right) \exp\left(\frac{-0.3i\cos(x)}{\epsilon}\right).$$

Here we test this initial data with the Mathieu potential $V = cos(y)$ [15]. The first eight Bloch eigenvalues for this potential are shown in Fig.8. We first do the initial Bloch decomposition with L^1 errors shown in Table 1, where $\Delta x = 2\pi/100$ and $\Delta k = 1/100$ have been used.

In our simulation, we use 10 bands. The eigen-structure indicates that caustics will appear in at least three bands. In Fig. 9 with 201×101 grid points, peaks correspond to turning points of the multi-valued velocities and valleys correspond to rarefaction waves.

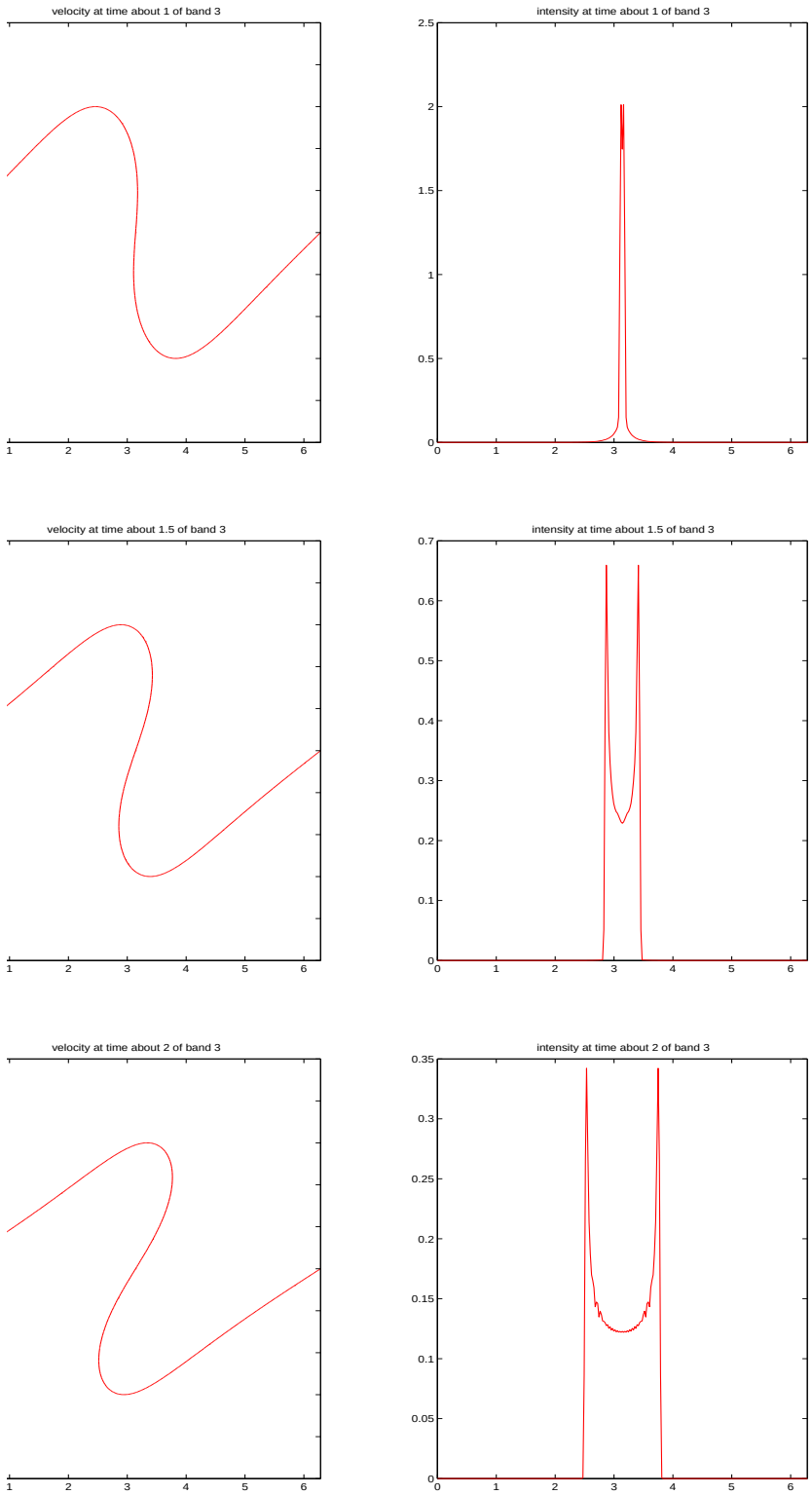

FIGURE 4. Example 2, $n = 3$, velocity and density at different times

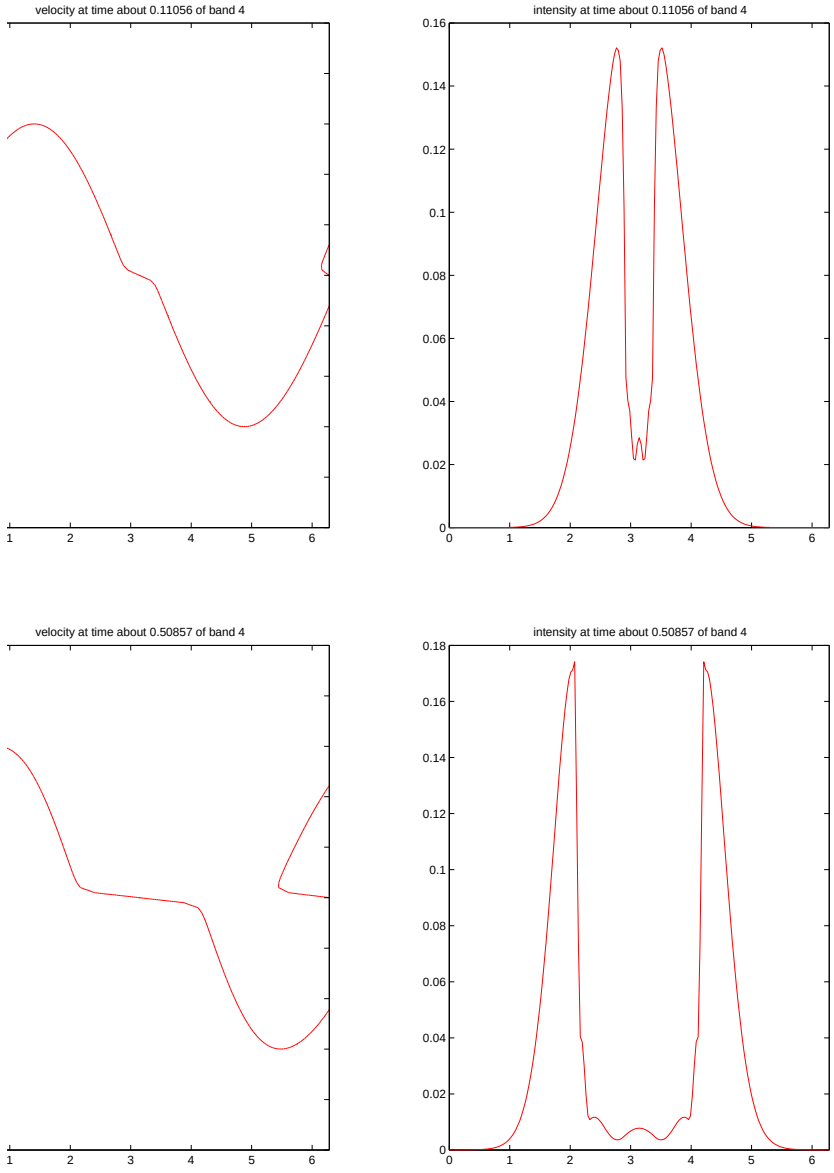

FIGURE 5. Example 2, $n = 4$, velocity and density at different time

ACKNOWLEDGMENTS

The authors thank the referees for their valuable comments and suggestions which have helped to improve the paper greatly. This research was partially supported by the National Science Foundation under Grant DMS05-05975 and the Kinetic FRG grant DMS07-57227.

REFERENCES

[1] J. Asch and A. Knauf. Motion in periodic potentials. *Nonlinearity*, 11(1):175–200, 1998.
[2] N. Ashcroft and N. Mermin. *Solid-state Physics*. Rinehart and Winston, Holt, 1976.

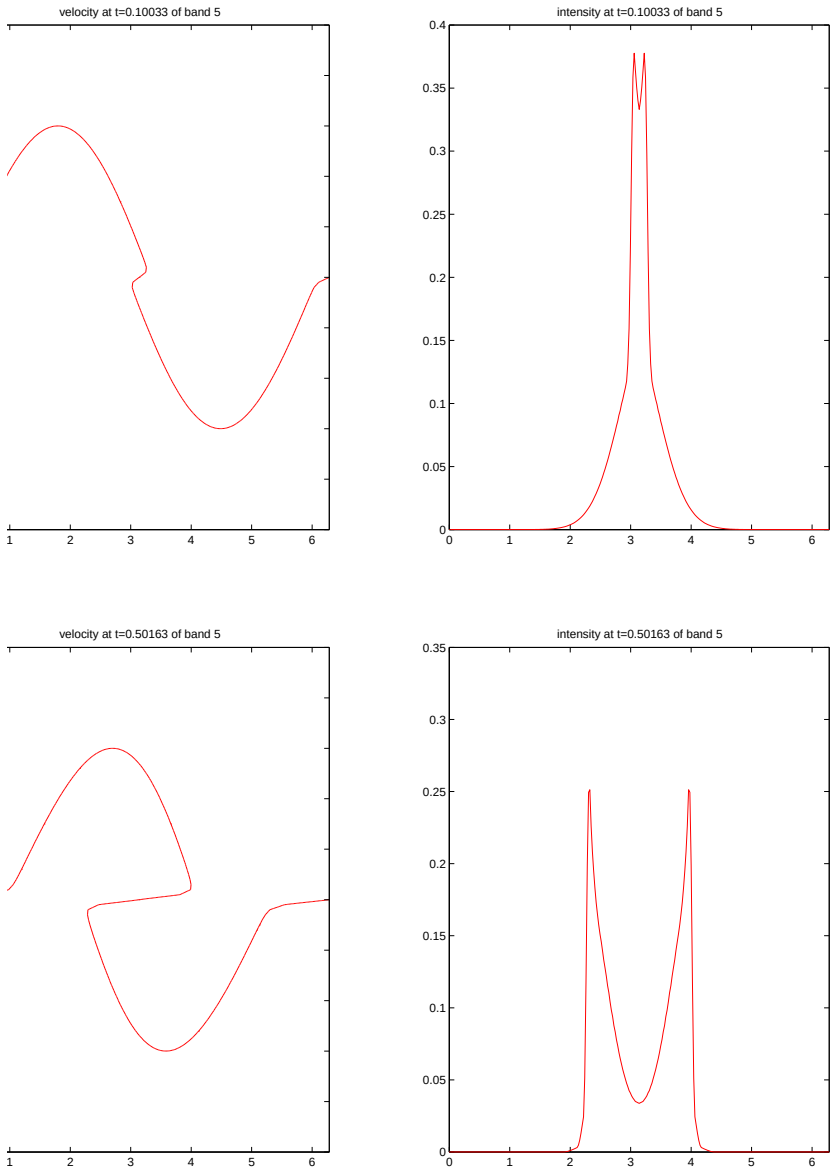

FIGURE 6. Example 2, $n = 5$, velocity and density of band 5 at different times

[3] G. Bal, A. Fannjiang, G. Papanicolaou, and L. Ryzhik. Radiative transport in a periodic structure. *J. Statist. Phys.*, 95(1-2):479–494, 1999.

[4] W. Bao, S. Jin, and P. A. Markowich. On time-splitting spectral approximations for the Schrödinger equation in the semiclassical regime. *J. Comput. Phys.*, 175(2):487–524, 2002.

[5] A. Bensoussan, J.-L. Lions, and G. Papanicolaou. *Asymptotic analysis for periodic structures*, volume 5 of *Studies in Mathematics and its Applications*. North-Holland Publishing Co., Amsterdam, 1978.

[6] F. Bloch. über die quantenmechanik dder elektronen in kristallgittern. *Z. Phys.*, 52:555–600, 1928.

[7] E. I. Blount. Formalisms of band theory. In *Solid State Physics, Vol. 13*, pages 305–373. Academic Press, New York, 1962.

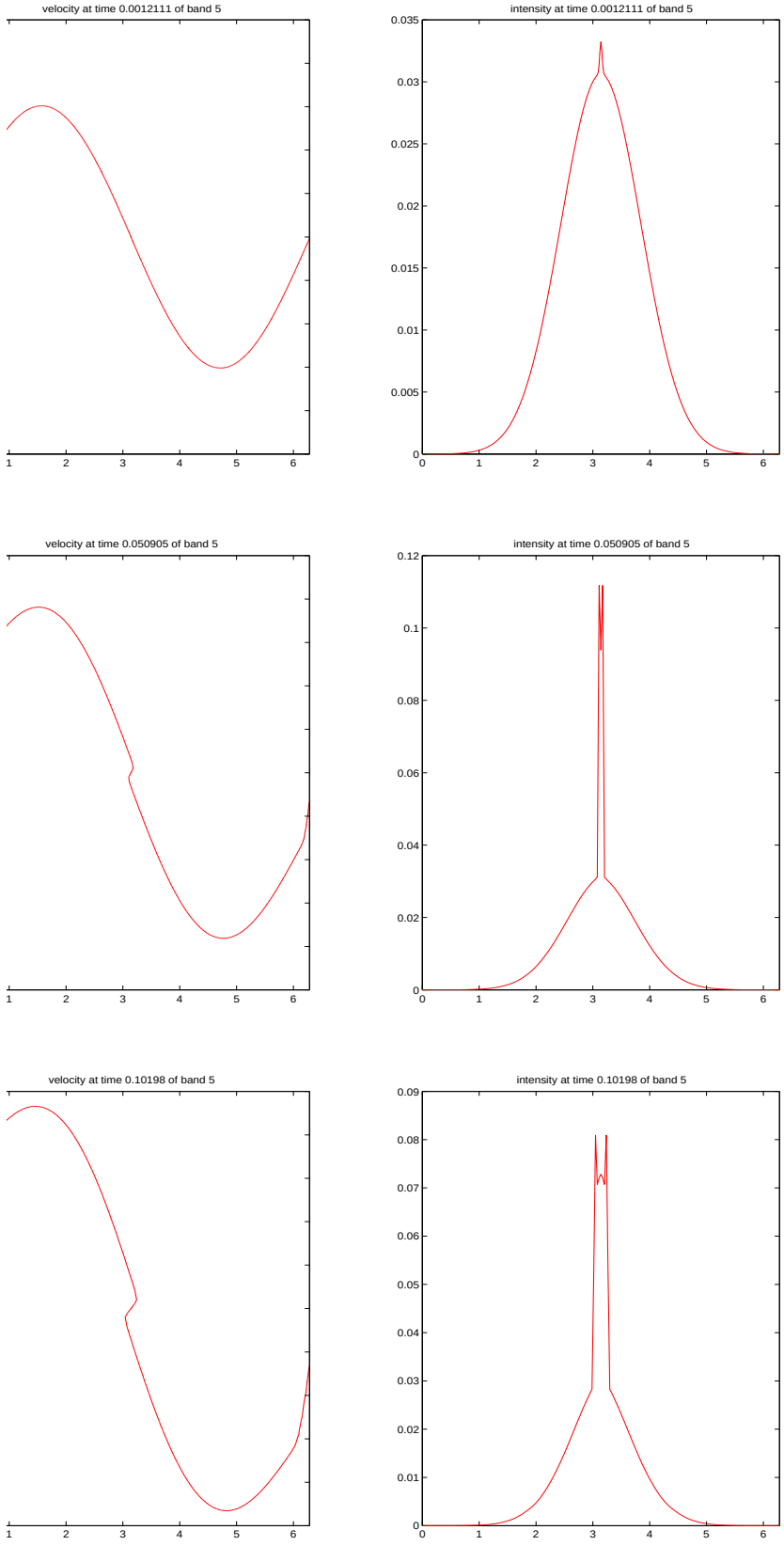

FIGURE 7. Example 3, velocity and density of band 5 with $V_e = \frac{|x-\pi|^2}{2}$ at different times

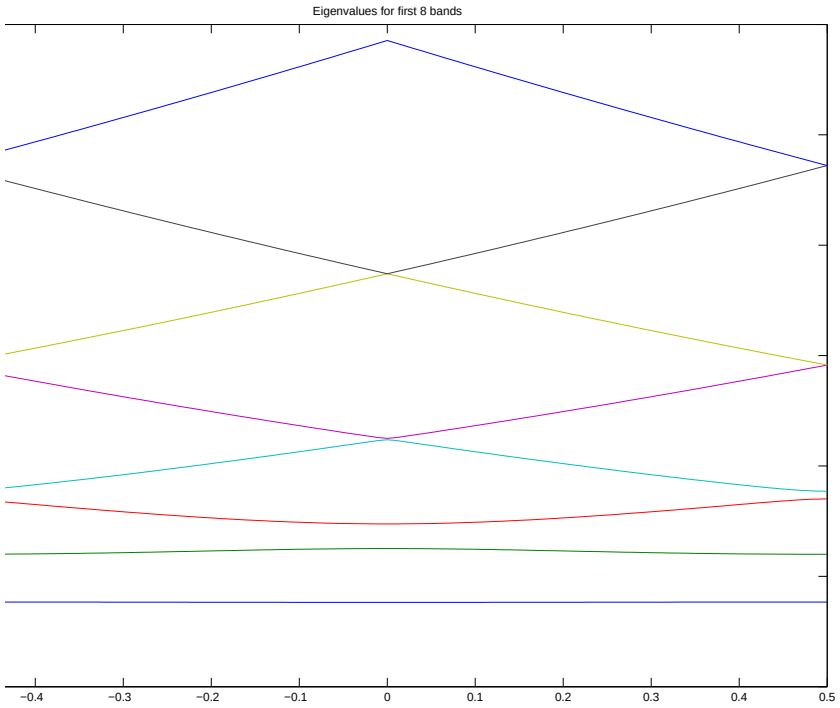

FIGURE 8. Eigenvalues for $V(y) = cos(y)$ and $b(y) = \frac{3}{2} + \sin(y)$ of band 1, 2, $\cdots$, 8 (bottom to top).

[8] L.-T. Cheng, H. Liu, and S. Osher. Computational high-frequency wave propagation using the level set method, with applications to the semi-classical limit of Schrödinger equations. *Commun. Math. Sci.*, 1(3):593–621, 2003.

[9] L.-T. Cheng, S. Osher, M. Kang, H. Shim, and Y.-H. R. Tsai. Reflection in a level set framework for geometric optics. *Computer Methods in Engineering and Physics*, 5(4), 2004.

[10] M. G. Crandall and P.-L. Lions. Viscosity solutions of Hamilton-Jacobi equations. *Trans. Amer. Math. Soc.*, 277(1):1–42, 1983.

[11] M. G. Crandall and P.-L. Lions. Two approximations of solutions of Hamilton-Jacobi equations. *Math. Comp.*, 43(167):1–19, 1984.

[12] B. Engquist, O. Runborg, and A.-K. Tornberg. High frequency wave propagation by the segment projection method. *J. Comput. Phys.*, 178(2):373–390, 2002.

[13] P. Gérard, P. A. Markowich, N. J. Mauser, and F. Poupaud. Homogenization limits and Wigner transforms. *Comm. Pure Appl. Math.*, 50(4):323–379, 1997.

[14] L. Gosse. Multiphase semiclassical approximation of an electron in a one-dimensional crystalline lattice. II. Impurities, confinement and Bloch oscillations. *J. Comput. Phys.*, 201(1):344–375, 2004.

[15] L. Gosse and P. A. Markowich. Multiphase semiclassical approximation of an electron in a one-dimensional crystalline lattice. I. Homogeneous problems. *J. Comput. Phys.*, 197(2):387–417, 2004.

[16] L. Gosse and N. J. Mauser. Multiphase semiclassical approximation of an electron in a one-dimensional crystalline lattice. III. From ab initio models to WKB for Schrödinger-Poisson. *J. Comput. Phys.*, 211(1):326–346, 2006.

[17] S. Gottlieb, C.-W. Shu, and E. Tadmor. Strong stability-preserving high-order time discretization methods. *SIAM Rev.*, 43(1):89–112 (electronic), 2001.

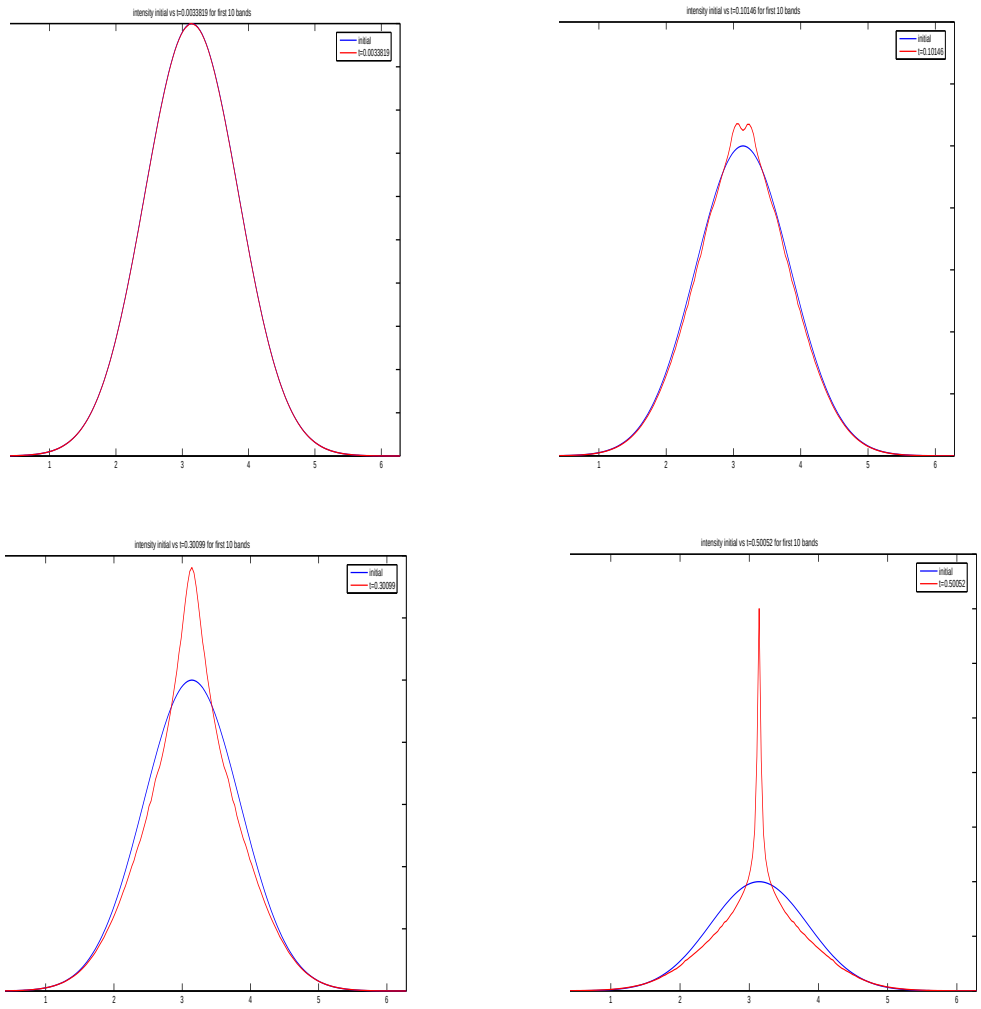

FIGURE 9. Example 4, total averaged density with 10 bands when $t = 0.003, 0.1$ in upper row (from left to right) and $t = 0.3, 0.5$ in bottom row.

[18] J.-C. Guillot, J. Ralston, and E. Trubowitz. Semi-classical approximations in solid state physics. In *Partial differential equations (Rio de Janeiro, 1986)*, volume 1324 of *Lecture Notes in Math.*, pages 263–269. Springer, Berlin, 1988.

[19] Z. Huang, S. Jin, P. A. Markowich, and C. Sparber. A Bloch decomposition-based split-step pseudospectral method for quantum dynamics with periodic potentials. *SIAM J. Sci. Comput.*, 29(2):515–538 (electronic), 2007.

[20] S. Jin, H. Liu, S. Osher, and Y.-H. R. Tsai. Computing multi-valued physical observables for the high frequency limit of symmetric hyperbolic systems. *J. Comput. Phys.*, 210(2):497–518, 2005.

[21] S. Jin, H. Liu, S. Osher, and Y.-H. R. Tsai. Computing multivalued physical observables for the semiclassical limit of the Schrödinger equation. *J. Comput. Phys.*, 205(1):222–241, 2005.

[22] S. Jin and S. Osher. A level set method for the computation of multivalued solutions to quasi-linear hyperbolic PDEs and Hamilton-Jacobi equations. *Commun. Math. Sci.*, 1(3):575–591, 2003.

[23] S. Jin and X. Yang. Computation of the semiclassical limit of the schrodinger equation with phase shift by a level set method. *J. Sci. Comput.*, 2007.

[24] P.-L. Lions and T. Paul. Sur les mesures de Wigner. *Rev. Mat. Iberoamericana*, 9(3):553–618, 1993.

[25] H. Liu, L.-T. Cheng, and S. Osher. A level set framework for capturing multi-valued solutions of nonlinear first-order equations. *J. Sci. Comput.*, 29(3):353–373, 2006.
[26] H. Liu, S. Osher, and Y.-H. R. Tsai. Multi-valued solution and level set methods in computational high frequency wave propagation. *Comm. Compu. Phys.*, 1(5):765–804, 2006.
[27] H. Liu and Z. Wang. Computing multi-valued velocity and electric fields for 1D Euler-Poisson equations. *Appl. Numer. Math.*, 57(5-7):821–836, 2007.
[28] H. Liu and Z. Wang. A fieled-space based level set method for computing mult-valued solutions to 1D Euler-Poisson equations. *J. Comput. Phys.*, 225:591–614, 2007.
[29] H. Liu and Z. Wang. Superposition of multi-valued solutions in high frequency wave dynamics. *Accepted by J. Sci. Comput.*, 2008.
[30] J. M. Luttinger. The effect of a magnetic field on electrons in a periodic potential. *Physical Rev. (2)*, 84:814–817, 1951.
[31] P. A. Markowich, N. J. Mauser, and F. Poupaud. A Wigner-function approach to (semi)classical limits: electrons in a periodic potential. *J. Math. Phys.*, 35(3):1066–1094, 1994.
[32] V. P. Maslov and M. V. Fedoriuk. *Semiclassical approximation in quantum mechanics*, volume 7 of *Mathematical Physics and Applied Mathematics*. D. Reidel Publishing Co., Dordrecht, 1981. Translated from the Russian by J. Niederle and J. Tolar, Contemporary Mathematics, 5.
[33] C. Min. Local level set method in high dimension and codimension. *J. Comput. Phys.*, 200(1):368–382, 2004.
[34] S. Osher, L.-T. Cheng, M. Kang, H. Shim, and Y.-H. R. Tsai. Geometric optics in a phase-space-based level set and Eulerian framework. *J. Comput. Phys.*, 179(2):622–648, 2002.
[35] S. Osher and J. A. Sethian. Fronts propagating with curvature-dependent speed: algorithms based on Hamilton-Jacobi formulations. *J. Comput. Phys.*, 79(1):12–49, 1988.
[36] G. Panati, H. Spohn, and S. Teufel. Effective dynamics for Bloch electrons: Peierls substitution and beyond. *Comm. Math. Phys.*, 242(3):547–578, 2003.
[37] D. Peng, B. Merriman, S. Osher, H. Zhao, and M. Kang. A PDE-based fast local level set method. *J. Comput. Phys.*, 155(2):410–438, 1999.
[38] J. Qian, L.-T. Cheng, and S. Osher. A level set-based Eulerian approach for anisotropic wave propagation. *Wave Motion*, 37(4):365–379, 2003.
[39] C. Sparber, P. A. Markowich, and N. J. Mauser. Wigner functions versus WKB-methods in multivalued geometrical optics. *Asymptot. Anal.*, 33(2):153–187, 2003.
[40] C. H. Wilcox. Theory of Bloch waves. *J. Analyse Math.*, 33:146–167, 1978.
[41] J. Zak. Dynamics of electrons in solids in external fields. *Phys. Rev.*, 1368:686–695, 1968.

Iowa State University, Mathematics Department, Ames, IA 50011
E-mail address: hliu@iastate.edu